Reaction Chemistry & Engineering

ROYAL SOCIETY OF CHEMISTRY

PAPER

View Article Online
View Journal

Cite this: DOI: 10.1039/d4re00235k

Boosting the kinetics of PET glycolysis†

Maria Schlüter,[ab] Ryota Enomoto,[a] Shin Makino,[a] Lisa Weihs,[c] Cyra Lina Stamm,[a] Kerstin Wohlgemuth [b] and Christoph Held *[ac]

Received 8th May 2024,
Accepted 2nd July 2024

DOI: 10.1039/d4re00235k

rsc.li/reaction-engineering

Glycolysis is the most promising chemical recycling method to depolymerize poly(ethylene terephthalate) (PET) with ethylene glycol (EG) into the monomer bis(2-hydroxyethyl) terephthalate (BHET). Boosting the depolymerization kinetics while staying under comparatively mild and green reaction conditions is required to bring glycolysis to industrial scale utilization. This work suggests achieving this goal by a combined pressure, temperature and co-solvent addition approach. By using the environmentally friendly γ-valerolactone (GVL) as a suitable co-solvent in the traditional PET glycolysis system, and slight temperature and pressure elevation, the kinetics was boosted by almost two orders of magnitude compared to the standard literature process. A kinetic model was employed to describe the kinetics as a function of temperature and GVL concentration. The optimized condition allowed nearly full conversion after 2 minutes only.

1. Introduction

Nowadays, poly(ethylene terephthalate) (PET) production is still comparably cheap, and PET's unrivalled functional properties – including strong mechanical, thermal, and chemical resistance, as well as dimensional stability[1–3] – make it an essential material for packaging on a global scale. Approximately 80% of the worldwide PET demand is attributed to the production of bottles.[4] Whereas in 2021, about 584 billion bottles were manufactured,[5] and this value is expected to double within the next two decades.[6] This will inevitably result in a substantial increase of post-consumer PET waste. Even today, effective strategies for managing high quality PET bottle waste streams have not yet been successfully implemented. Most existing mechanical recycling methods lead to the downcycling of the input material into products such as textiles or fibers, caused by thermal and hydrolytic degradation in each recycling loop.[7,8] Ultimately, these materials often end up being land-filled or incinerated. This open-loop recycling approach is unsustainable, necessitating the exploration of more viable solutions for recycling post-consumer PET materials. Chemical recycling offers a promising alternative, wherein PET waste can be broken down into its monomeric building blocks, yielding high-quality PET through re-polymerization. Additionally, using chemical recycling overcomes the disadvantageous effect of impurities on mechanical recycling to avoid downcycling products, thereby achieving closed-loop PET recycling.[9] Chemical recycling is realized by contacting PET with a solvent, which acts also as a reactant. Methanol might be used, but it requires relatively high temperatures (up to 280 °C) and high pressures (20–40 bar).[10–13] Hydrolysis requires very acidic or basic conditions, leading to severe equipment corrosion and large amount of acid and alkali wastewater.[14–19] In contrast, using ethylene glycol ("PET glycolysis") has emerged as one of the most promising methods for chemical recycling of PET, due to the rather mild reaction conditions, employment of less volatile and non-toxic reagents and a minimal number of waste streams. A PET repeating unit (ru) reacts with ethylene glycol (EG) into the monomer bis(2-hydroxyethyl) terephthalate (BHET) (see Fig. 1), which is a slightly endothermic reaction.[20]

Nearly full conversion is achievable in PET glycolysis above 170 °C,[20,21] but reaction kinetics is one of the bottlenecks to bring PET glycolysis towards a commercial scale. Reaction kinetics is influenced by the type and

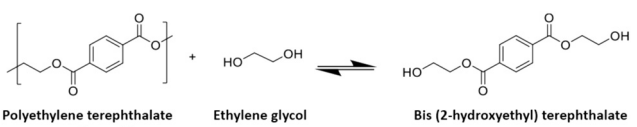

Fig. 1 Depolymerization reaction of PET with EG into BHET.

[a] TU Dortmund University, Department of Biochemical and Chemical Engineering, Laboratory of Fluid Separations, 44227 Dortmund, Germany.
E-mail: christoph.held@tu-dortmund.de; Tel: +49 231 755 2086
[b] TU Dortmund University, Department of Biochemical and Chemical Engineering, Laboratory of Plant and Process Design, 44227 Dortmund, Germany
[c] TU Dortmund University, Department of Biochemical and Chemical Engineering, Laboratory of Thermodynamics, 44227 Dortmund, Germany

† Electronic supplementary information (ESI) available. See DOI: https://doi.org/10.1039/d4re00235k

concentration of catalyst, PET particle size, concentration of reactants and temperature as well as using co-solvents that serve as kinetic activators. The homogeneous metal acetate catalyst zinc acetate ($ZnAc_2$) has proven to be a reliable depolymerization catalyst, providing good selectivity towards BHET.[21–24] The most common studies investigate PET glycolysis at 190 °C, since higher temperatures will cause significant EG evaporation. Nevertheless, there are some studies at temperatures up to 275 °C, which was achieved by pressurizing the reaction mixtures.[25,26] Another strategy to increase kinetics is the addition of co-solvents to the initial reaction mixture, such as aniline, nitrobenzene, 1-methyl-2-pyrrolidinone, and dimethyl sulfoxide (DMSO) or a 1,3-dimethylurea (1,3-DMU)/$ZnAc_2$ deep eutectic solvent system.[27,28] Recently, Le *et al.*[29] reported beneficial effects of the green solvent anisole on the kinetics.

Based on a reference kinetic dataset, which we determined for the $ZnAc_2$-catalysed PET glycolysis at 190 °C and 1 bar, the objectives of this study are to: first, improve kinetics by using the biomass-derived green platform molecule γ-valerolactone (GVL)[30] as additional co-solvent in the traditional reaction mixture. Moreover, individual experiments were performed to understand the kinetic boost of GVL in detail. Second, increase kinetics by elevating the temperature without solvent loss, which we will achieve by increasing the pressure. Third, make use of the combined effect of GVL as co-solvent and a temperature increase to ultimately boost the reaction kinetics. The influence of these individual factors on the reaction kinetics was evaluated by kinetic constants, obtained by the pseudo-first order reversible reaction model, as utilized in other studies.[20,31,32] This combined temperature and co-solvent optimization approach will achieve a kinetic boost of PET glycolysis of about two orders of magnitude over the conventional process, thus contributing to a greener chemical recycling strategy.

2. Experimental section

Comprehensive information regarding the set-up, preparation, procedure and evaluation of the experiments performed in this study as well as descriptions of the analytical methods applied is available in the ESI.†

2.1 Materials

Table 1 presents a list of the chemicals used in this study, along with their purities.

The PET used in this study was sourced from colorless single-use post-consumer bottles. Caps and labels were taken off and surface impurities were removed using small amounts of acetone. The remaining material was manually cut into 5 × 5 × 0.2 mm pieces. Following this, the PET particles were shred into small particles using a grinder. These crushed PET particles underwent fractionation in a sieving tower. Unless otherwise stated, the experiments were carried out with a particle size fraction of $0.2 \leq d_p < 1$ mm.

2.2 Sample preparation for PET glycolysis kinetic investigations

The experiments were conducted in 20 ml glass vials acting as batch reactors, with each vial containing approximately 0.65 g of PET. The relatively small PET particle size ($0.2 \leq d_p < 1$ mm) was chosen to facilitate homogeneous mixing of the reactants in the small glass vial reactors. Following PET addition, a specific quantity of $ZnAc_2$/EG catalyst solution was added into each vial, along with pure EG and, when investigated, GVL. The molar ratio of the PET's repeating unit to $ZnAc_2$ $\left(\frac{n^0_{PETru}}{n_{ZnAc_2}}\right)$ was set to 50, and the initial mass ratio of solvent to PET $\left(\frac{m^0_{EG} + m_{GVL}}{m^0_{PET}}\right)$ was maintained at 6. Finally, a small magnetic stirrer was added.

2.3 Set-up and procedure for PET glycolysis kinetic investigations

The depolymerization reactions were performed using a magnetic hot plate stirrer equipped with a cylindrical alumina heating block preheated to the desired temperature. Sample vials, including the catalyst, were prepared under ambient conditions and placed in the preheated aluminum block with stirring at 1400 rpm. Following a three-minute dead time required to reach the desired reaction temperature, the reaction time commenced. After the designated reaction time, samples were withdrawn and cooled to 90 °C. Subsequently, they were filled with 14 ml of

Table 1 Characteristics of chemicals used in this work

Chemical	Abbreviation	CAS	M/g mol^{-1}	Supplier	Type	Purity/wt%
Poly(ethylene terephthalate)	PET	25038-59-9	58 000[a]	Colorless single-use post-consumer bottles ("JA")		
Ethylene glycol	EG	107-21-1	62.07	Sigma-Aldrich	ReagentPlus	99
Zinc acetate	$ZnAc_2$	557-34-6	183.48	Sigma-Aldrich		99.99
γ-Valerolactone	GVL	108-29-2	100.12	Sigma-Aldrich	ReagentPlus	99
Water	H_2O	7789-18-5	18.015	Deionized		
Acetone	—	67-64-1	58.08	VWR international	TECHNICAL	99
Bis(2-hydroxyethyl) terephthalate	BHET	959-26-2	254.238	Sigma-Aldrich		98.1
Methanol	—	67-56-1	32.04	VWR international	HiPerSolv	99.8

[a] Mass average molecular weight determined by the ASTM D 4603 standard test method in a previous work.[33]

hot (90 °C) water, followed by filtration to separate the solid residual fraction, primarily unconverted PET, and the liquid filtrate fraction, mainly composed of BHET, EG, water, $ZnAc_2$ and, when investigated, GVL. PET conversion X_{PET} was determined using eqn (1), based on the mass of the retrieved dried (60 °C) unconverted PET m_{PET} related to the initial PET mass m^0_{PET}.

$$X_{PET} = \frac{m^0_{PET} - m_{PET}}{m^0_{PET}} \cdot 100 \quad (1)$$

The BHET process yield $Y^{process}_{BHET}$ (see eqn (2)) was calculated based on the mass ratio of the final BHET product (crystallized at 6 °C and dried at 60 °C) over the initially weighed PET.

$$Y^{process}_{BHET} = \frac{m_{BHET}/M_{BHET}}{m^0_{PET}/M_{PETru}} \cdot 100 \quad (2)$$

2.4 Analytical quantification of glycolysis products

Differential Scanning Calorimetry (DSC) was employed for dried PET residue samples to determine the melting temperature and enthalpy of the solid. High Performance Liquid Chromatography (HPLC) was employed to determine the mole fraction of monomer in the final monomer/dimer product samples. For more information: see the ESI† section A.4.

3. Kinetic model

A detailed description of the kinetic modeling can be found in section B in the ESI.† As can be seen from Fig. 1, the reversible PET glycolysis reaction can be modeled as the reaction of one mole of PET's repeating unit with one mole of EG giving one mole of BHET monomer. The change of the mole fractions x_i of the reactants i along the reaction coordinate can be described *via* eqn (3).

$$\frac{dx_{PETru}}{dt} = \frac{dx_{EG}}{dt} = -\frac{dx_{BHET}}{dt} = -k \cdot x_{PETru} \cdot x_{EG} + \frac{k}{K_x} \cdot x_{BHET} \quad (3)$$

K_x describes the equilibrium (eq) composition of the reaction mixture and is defined in the following eqn (4).

$$K_x = \frac{x^{eq}_{BHET}}{x^{eq}_{PETru} \cdot x^{eq}_{EG}} \quad (4)$$

The set of differential equations (eqn (3)) was solved using Matlab™'s ODE15s solver, with the initial composition of the reactants serving as the initial condition. Simultaneously, using Matlab™'s internal function lsqcurvefit, the kinetic constant k was retrieved from the experimental data obtained in this study.

4. Results and discussion

Zinc acetate-catalysed PET glycolysis operates *via* the Lewis acid reaction mechanism. The process initiates with PET activation, as the Lewis acid catalyst engages with the carbonyl oxygen of the PET polymer, facilitating ester bond cleavage. This activation step weakens the bond between the carbonyl carbon and the ester group oxygen. Subsequently, the activated PET molecule undergoes nucleophilic attack by EG, with the hydroxyl group of EG targeting the activated carbonyl carbon of PET. This yields a tetrahedral intermediate. Following this, the ring opening of the tetrahedral intermediate takes place, ultimately resulting in the formation of the BHET monomer.[34] In this work, kinetic data series were obtained according to the conditions in Table 2, whereby series 1 represents the standard literature process at 1 bar, 190 °C without co-solvent, serving as a reference in this study.

Table S2 in the ESI† summarises the experimental and modeling results of all kinetic experiments. The experimental results include the approximate reaction time until reaching the reaction equilibrium t^{eq}, the determined equilibrium conversion X^{eq}_{PET}, the equilibrium composition of the reaction mixture K_x, the BHET process yield at the

Table 2 Overview of conducted experimental kinetic series in this work with constant parameters of: $\frac{n_{PETru}}{n_{ZnAc_2}} = 50$, $0.2 \leq d_p < 1$ mm and a stirrer speed of 1400 rpm

Objective	Series no.	Symbol	$\frac{m_{GVL}}{m^0_{EG}}$/g g^{-1}	$\frac{m^0_{EG}+m_{GVL}}{m^0_{PET}}$/g g^{-1}	$\frac{m^0_{EG}}{m^0_{PET}}$/g g^{-1}	p/bar	T/°C
Reference	1	■	0	6	6	1	190
GVL influence	2	●	0.118	6	5.36	1	190
	3	▲	0.236	6	4.85	1	190
	4	▼	0.473	6	4.07	1	190
Temperature influence	5	◆	0	6	6	2	215
	6	●	0	6	6	3	232
Combined influence of GVL and temperature	7	◆	0.118	6	5.36	3	232

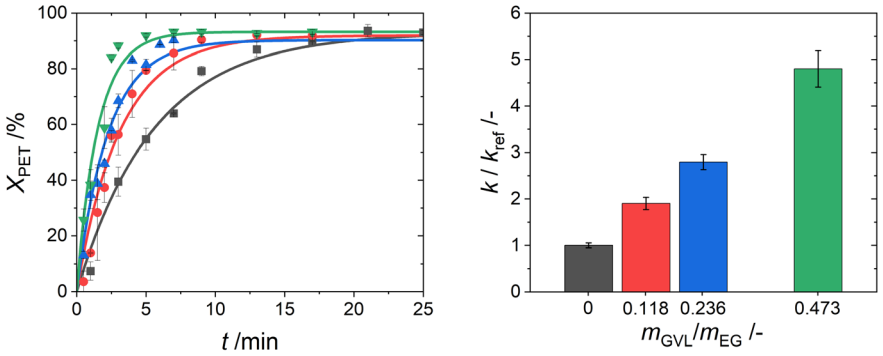

Fig. 2 (a) PET conversion X_{PET} over reaction time t for different GVL ratios. Experimental data (symbols) *vs.* modeling (lines) using eqn (1), (3) and (4); (b) kinetic constants k obtained from the pseudo-first order reversible reaction model (eqn (3)) applied to the kinetic experiments with respect to the reference kinetic series k_{ref} with $\frac{m_{GVL}}{m^0_{EG}}$ of 0 (grey = reference), 0.118 (red), 0.236 (blue) and 0.473 (green). Other reaction conditions are: T = 190 °C, p = 1 bar, $\frac{m^0_{EG}+m_{GVL}}{m^0_{PET}}$ = 6, $\frac{n_{PETru}}{n_{ZnAc_2}}$ = 50, 0.2 ≤ d_p < 1 mm and a stirrer speed of 1400 rpm. A detailed summary of all results can be found in Table S2.†

reaction equilibrium $Y^{process,eq}_{BHET}$ and the monomer mole fraction $x^{product}_{Monomer}$ in the BHET product. Regarding the modeling, Table S2† contains the initial composition of the reaction mixture as well as the retrieved values for the kinetic constants k. In addition to the kinetic investigations in Table S2,† individual experiments were conducted to gain a detailed understanding of the kinetic enhancement provided by GVL.

4.1 GVL influence on reaction kinetics

Maintaining reference conditions at 1 bar and 190 °C, the first investigation focused on the sole impact of varying amounts of the co-solvent GVL on the reaction kinetics. Fig. 2 (a) presents the results of the PET conversion over time for the kinetic series 1–4 (numbering according to Table 2). Fig. 2 (b) illustrates the specific kinetic constants in relation to the reference kinetic series 1.

It becomes evident from Fig. 2 (a) that the reaction mixture without GVL required approximately 21 minutes to achieve an equilibrium conversion of around 93%. In comparison to other PET glycolysis reactions catalysed by $ZnAc_2$, this reaction kinetics is already fast. This is attributed to the small-sized PET particles (0.2 ≤ d_p < 1 mm) used in our approximately 3.5 ml reaction mixture. Notably, the same equilibrium conversion was reached much faster by using GVL co-solvent without influencing the reaction equilibrium, *i.e.* still allowing nearly full conversion. Further, boiling of the liquid phase during the experiments was not observed probably due to the high boiling temperature of GVL (205 °C at 1 bar (ref. 35)) and the absence of any influencing temperature minimum azeotrope between EG and GVL under the investigated conditions. Besides, Fig. 2 (a) illustrates the results of the kinetic modeling, wherein the kinetic constant k was retrieved from the experimental data using K_x from experimental data obtained at the reaction equilibrium (see Table S2 in the ESI†). For a more detailed understanding of the kinetic model, Fig. S3 in the ESI† displays the changing mole fractions of the components during depolymerization over reaction time for experimental series 4 $\left(\frac{m_{GVL}}{m^0_{EG}} = 0.473\ g\ g^{-1}\right)$ with the highest amount of GVL, where EG was present still in excess. Consequently, the concentration of EG barely changes along the progressing reaction time (according to reviews from paper 3) (−2.12%). That is why the reaction can be categorized as a pseudo-first order reversible reaction even at highest studied GVL concentrations.

Additionally, Fig. 2 (b) provides an overview of the obtained kinetic constants in relation to the reference kinetic series. The kinetic constant increases linearly with the higher GVL/EG ratio in the mixture. A ratio $\frac{m_{GVL}}{m^0_{EG}}$ of 0.118 already doubles the kinetic constant, and a ratio of 0.473 increases the value by nearly five times compared to the reference k. These values underline the accelerating effect of GVL on the reaction kinetics at isothermal and isobaric conditions (190 °C, 1 bar).

4.2 Temperature influence on reaction kinetics

Temperature is known to impact reaction kinetics. At ambient pressure, a temperature of about 190 °C must not be exceeded to avoid EG evaporation. Thus, temperature increase requires elevated pressure. To exclude a pressure influence on reaction kinetics, the influence of pressure on reaction kinetics at isothermal temperature of 190 °C was analyzed. The results are illustrated in Fig. S4 in the ESI.† It can be concluded that a pressure increase to 2 bar and 3 bar did not significantly influence the reaction kinetics nor the reaction equilibrium of the PET glycolysis reaction compared to the reference condition (190 °C, 1 bar). The maximum

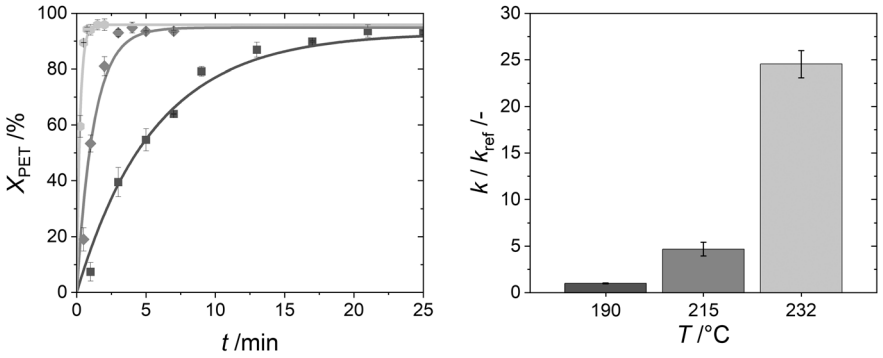

(a) (b)

Fig. 3 (a) PET conversion X_{PET} over reaction time t for different pressures and temperatures. Experimental data (symbols) *vs.* modeling (lines) using eqn (1), (3) and (4); (b) kinetic constants k obtained from the pseudo-first order reversible reaction model (eqn (3)) applied to the kinetic experiments with respect to the reference kinetic series k_{ref} with T = 190 °C & p = 1 bar (dark grey = reference), T = 215 °C & p = 2 bar (mid-grey) and T = 232 °C & p = 3 bar (light grey). Other reaction conditions are: $\frac{m_{GVL}}{m^0_{EG}} = 0$, $\frac{m^0_{EG} + m_{GVL}}{m^0_{PET}} = 6$, $\frac{n_{PETru}}{n_{ZnAc_2}} = 50$, $0.2 \leq d_p < 1$ mm and a stirrer speed of 1400 rpm. A detailed summary of all results can be found in Table S2.†

reaction temperatures to avoid EG evaporation at 2 bar and 3 bar were estimated based on the vapor pressure curve of EG (Fig. S5 in the ESI†) minus an additional temperature difference of 7 K. The resulting reaction temperatures were 215 °C (2 bar) and 232 °C (3 bar). The results of reaction series no. 5 and 6 are compared in Fig. 3 (a) with the reference conditions. Additionally, Fig. 3 (b) provides an overview of the specific kinetic constants in relation to the reference kinetic series.

As expected, the pressure-assisted temperature increase accelerated the reaction, whereby the elevated reaction temperatures were reached after the dead time of 3 minutes, as can be seen in Fig. S2 in the ESI.† The temperature increase had also a slight effect on the reaction equilibrium of the endothermic reaction because the mean equilibrium conversion increased from 93 over 93.5 to 96%. Additionally, Fig. 3 (a) shows the results of the kinetic modeling using eqn (1), (3) and (4), wherein the kinetic constant k was retrieved from the experimental data using K_x from experimental data obtained at the reaction equilibrium (see Table S2 in the ESI†). The modeled and experimental data exhibit good agreement, reinforcing the characterization of the reaction as a pseudo-first order reversible reaction, as described in the previous section.

Fig. 3 (b) also provides an overview of all kinetic constants in relation to the reference kinetic series. A 25-fold increase with respect to the reference kinetic series for a temperature of 232 °C at a pressure of 3 bar underlines the substantial temperature effect on the reaction kinetics as known from the Arrhenius approach.

4.3 Combined temperature and GVL influence on reaction kinetics

In the preceding sections, it was evaluated that the individual influences of GVL and temperature (assisted by pressurizing) independently accelerated the reaction kinetics. Building on this observation, we conducted an illustrative exploration of the combined effect of the temperature increase and GVL addition. Therefore, a relatively modest ratio $\frac{m_{GVL}}{m^0_{EG}}$ of 0.118 was selected, and a temperature of 232 °C at 3 bar was applied as can be seen in Table 2, reaction series no. 7. Fig. 4 (a) presents the results of the PET conversion over time for this kinetic series, along with the reference kinetic series 1 and the optimal outcomes derived from the individual effects of GVL (series 4) and temperature (series 6) on the kinetics according to Table 2. Fig. 4 (b) provides an overview of the specific kinetic constants in relation to the reference kinetic series 1.

Evidently, from Fig. 4, it can be concluded that introducing a small quantity of GVL into the mixture, and simultaneously elevating the reaction conditions to 232 °C at 3 bar, whereby the reaction temperature was reached after the dead time of 3 minutes, (see Fig. S2 in the ESI†) allowed for a 70-fold increase in reaction kinetics over the reference conditions. Just after 15 seconds of reaction time, the first sample of kinetic series 7 reached a near-equilibrium state. Because experimental data was not available between the reaction times of 0 and 15 seconds, fitting the kinetic constant k using K_x from experimental data obtained at the reaction equilibrium (see Table S2 in the ESI†) might not be that accurate. Nonetheless, the primary objective of the model in this study is to quantify the acceleration of the reaction kinetics through the kinetic constant. However, all obtained experimental data points align closely with the respective modeled kinetic curve in Fig. 4 (a). The significant amplification of almost two orders of magnitude relative to the reference kinetic series shown in Fig. 4 (b) underlines the substantial impact of temperature increase on the GVL-assisted PET glycolysis reaction.

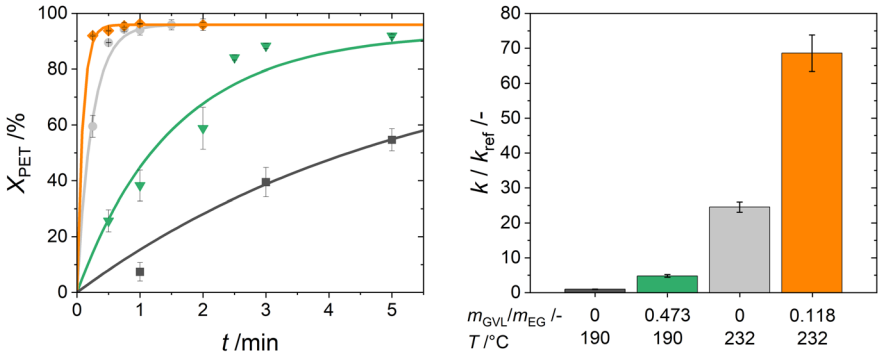

Fig. 4 (a) PET conversion X_{PET} over reaction time t for different temperatures, pressures and GVL ratios. Experimental data (symbols) *vs.* modeling (lines) using eqn (1), (3) and (4); (b) kinetic constants k obtained from the pseudo-first order reversible reaction model (eqn (3)) applied to the kinetic experiments with respect to the reference kinetic series k_{ref} with T = 190 °C & p = 1 bar & $\frac{m_{GVL}}{m^0_{EG}}$ = 0 (dark grey = reference), T = 190 °C & p = 1 bar & $\frac{m_{GVL}}{m^0_{EG}}$ = 0.473 (green), T = 232 °C & p = 3 bar & $\frac{m_{GVL}}{m^0_{EG}}$ = 0 (light grey) and T = 232 °C & p = 3 bar & $\frac{m_{GVL}}{m^0_{EG}}$ = 0.118 (orange). Other reaction conditions are: $\frac{m^0_{EG}+m_{GVL}}{m^0_{PET}}$ = 6, $\frac{n_{PETru}}{n_{ZnAc_2}}$ = 50, 0.2 ≤ d_p < 1 mm and a stirrer speed of 1400 rpm. A detailed summary of all results can be found in Table S2.†

4.4 Influence of increased reaction temperature and GVL on the reaction products and process yield

As outlined in section 2.4 (with further details provided in section A.4 of the ESI†), random samples of solid residues from the experimental kinetic series 1–6 were analyzed in HPLC and DSC. In terms of the sole impact of varying amounts of GVL (see section 4.1), HPLC analysis indicated a reduction of the monomer fraction in the product, from approximately 95 mol-% without GVL to 92 mol-% with the highest GVL concentration investigated in this study. Nevertheless, the final product predominantly comprised of BHET monomers, supporting the applied simplified model and neglecting the dimer equilibrium reaction. Further, analysis of an exemplary remaining liquid phase after BHET filtration was performed (see Fig. S8 in the ESI†). Neither the solid product nor the liquid phase revealed other reaction products, which might have been formed due to a reaction of $ZnAc_2$ with GVL. Additionally, the DSC analysis of random PET residue samples (Fig. S10 in the ESI†) detected mainly PET and no BHET monomer. However, with increasing GVL amount, a recognisable peak at the dimer melting temperature occurred, underlining the increased dimer formation through GVL. Random BHET crystals obtained from the elevated temperature kinetic series (see section 4.2) were also analyzed *via* HPLC. Detailed results are available in the ESI† (Fig. S7). It can be concluded that the obtained product crystals mainly consisted of BHET monomers (>95 mol-%) with small amounts of BHET dimers. The dimer mole fraction in the product did not significantly change upon temperature increase. Additionally, based on DSC results, the obtained PET residue comprised unconverted PET, with neither BHET monomer nor dimer found in the filtered PET residues (see Fig. S10 in the ESI†).

In order to evaluate the overall PET glycolysis process, the BHET process yield (see eqn (2)) at the reaction equilibrium was determined for all kinetic experimental series (see Table 2) conducted in this work. Values of about 80% were determined for the reference series no. 1 (190 °C, 1 bar), as well as for series no. 5 and 6 due to identical liquid composition of EG and H_2O in the downstream process, as anticipated. Comparable literature processes also yielded values ranging between 75 and 82%.[20,27,28] Apart from the beneficial effect of GVL on the kinetics, the overall process yield obtained from maximum conversion samples decreased from about 80% without GVL to 55% with the highest amount of GVL investigated in this study. This decline is attributed to the increasing fraction of GVL in the liquid phase of the downstream process and the enhanced solubility of BHET in GVL.[33]

4.5 Analysis of the reasons behind the GVL effect on the kinetics

Explanations for the accelerating effect of GVL on the kinetics can be broken down to three hypotheses: first, GVL accelerates the dissolution rate of PET. Second, GVL positively influences the molecular interactions between the reactants. Third, GVL enhances the catalyst activity. Following the first hypothesis, decoupling the impact of PET dissolution on reaction kinetics was needed. Therefore, three distinct experimental procedures as described in section A.5 in the ESI† were implemented. The results are summarized in Fig. 5.

It can be observed from Fig. 5 that there were no significant differences in the results concerning X_{PET} among the three procedures. Please note that all samples had the same composition of reactants and solvents as well as the same reaction time. This is a surprising effect

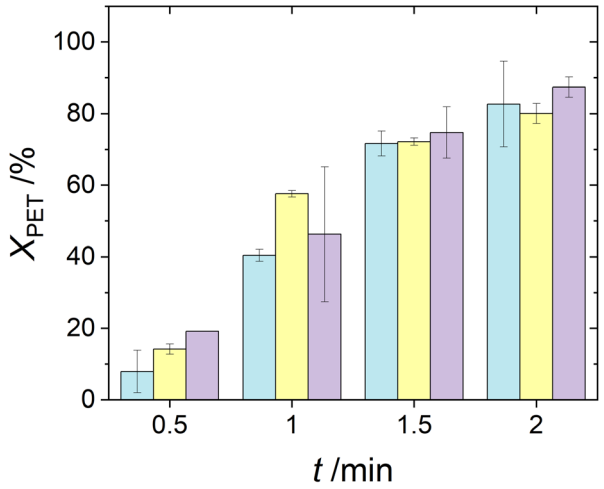

Fig. 5 PET conversion X_{PET} over reaction time t for different experimental procedures. Conventional procedure of putting complete prepared samples in the heating block and setting the dead time due to heating-up to 3 minutes (cyan); pre-heating the solvents and $ZnAc_2$ at the reaction temperature prior to PET dosage and using no dead time (yellow); pre-dissolving PET in GVL[36] prior to adding pre-heated $ZnAc_2$/EG catalyst solution and using no dead time (purple). Reaction conditions were $\frac{m_{GVL}}{m^0_{EG}}$ = 0.946, $\frac{m^0_{EG}}{m^0_{PET}}$ = 6, T = 190 °C, p = 1 bar, $\frac{n_{PETru}}{n_{ZnAc_2}}$ = 50, PET flakes = 5 × 5 × 0.2 mm and a stirrer speed of 1400 rpm adapted from Chen *et al.*[36] and modified to enable complete dissolution of PET in GVL.

contrary to the expectations and experience from the literature.[27] These experiments disproved the first hypothesis. Continuing with the remaining hypothesis, we know from other works ("Activity-Based Models to Predict Kinetics of Levulinic Acid Esterification"[37]) that co-solvents manipulate the thermodynamic activity of the reactants and the catalysts. Hence, we postulate based on the results from Fig. 5 that GVL has a beneficial effect on the activity of $ZnAc_2$, EG or PET. Following hypothesis three, we conducted experiments without the $ZnAc_2$ catalyst with and without GVL in the reaction system. To ensure a measurable conversion within a reasonable timeframe, samples were measured at 232 °C and 3 bar as described in sections 2.2 and 2.3. The conversion of the samples was compared after 7 minutes of reaction time and the results are depicted in Fig. 6.

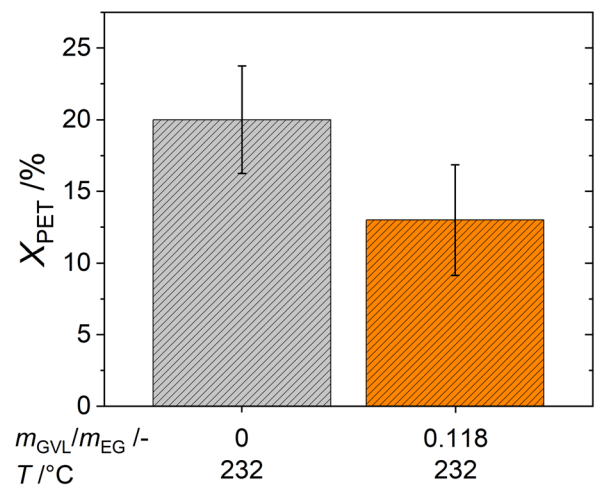

Fig. 6 PET conversion X_{PET} of samples without catalyst after 7 minutes of reaction time without GVL (light grey shaded) and with $\frac{m_{GVL}}{m^0_{EG}}$ = 0.118 (orange shaded) at T = 232 °C, p = 3 bar, $\frac{m^0_{EG}+m_{GVL}}{m^0_{PET}}$ = 6, 0.2 ≤ d_p < 1 mm and a stirrer speed of 1400 rpm.

Under the same reaction conditions, a 20% conversion was achieved without GVL, whereas only a 13% conversion was attained for the samples with GVL. The results obtained without the catalyst suggest that the enhanced kinetics due to the presence of GVL in the reaction mixture is not attributed to the interaction of GVL with the reactants. Instead, they are more likely attributed to the interaction between GVL and the $ZnAc_2$ catalyst, possibly involving acid–base synergistic catalysis.[34] Detailed descriptions of reaction mechanisms involving systems containing $ZnAc_2$/Lewis base catalysts in PET glycolysis have already been published in the literature.[28,34,38,39] Applied to our Lewis acid ($ZnAc_2$) catalysed reaction system, it is plausible that GVL functions as a Lewis base. This is because the oxygen atom in the lactone ring has a lone pair of electrons, which can be donated to form a bond with the electron-deficient species (Lewis acid). Consequently, GVL can coordinate with $ZnAc_2$ to promote bond cleavage and catalytic activity.

5. Conclusion and outlook

The aim of this study was to enhance the kinetics of the PET glycolysis reaction while maintaining comparatively mild reaction conditions. To quantify the acceleration of the reaction kinetics, the pseudo-first order reversible reaction model was employed by fitting the kinetic constant to the obtained experimental data. Under the reference condition of 190 °C and 1 bar, the impact of the biomass-derived green platform chemical GVL on the kinetics of the PET glycolysis was examined. Successfully, the reaction with a GVL to EG ratio $\frac{m_{GVL}}{m^0_{EG}}$ of 0.473 accelerated the reaction by a factor of about 5 with respect to the reference kinetic series. Furthermore, it was concluded that the enhanced kinetics due to the presence of GVL in the reaction mixture is attributed to the interaction between $ZnAc_2$ and GVL possibly due to acid–base synergistic catalysis. Apart from that, the influence of slightly elevated reaction conditions in terms of temperature and pressure was explored. The temperature increase assisted by pressure elevation markedly accelerated the reaction, with 5 times the acceleration at 215 °C and 25 times the acceleration at 232 °C, underscoring the substantial temperature effect on the reaction kinetics. Lastly, the combined temperature increase on the GVL-assisted PET glycolysis reaction was assessed. At a temperature of 232 °C,

pressure of 3 bar and a relatively small GVL to EG ratio $\frac{m_{GVL}}{m^0_{EG}}$ of 0.118, a 70-fold amplification relative to the reference kinetics was achieved. This emphasizes the positive combined effect on the reaction kinetics of all the influencing factors investigated in this study. All investigated approaches significantly decreased the reaction time of the PET glycolysis while staying under comparatively mild reaction conditions, thus contributing to a greener PET glycolysis reaction. Nevertheless, further investigations are required regarding the downstream of the PET glycolysis process. While only elevating the temperature and pressure does not affect the downstream process, the introduction of GVL presents a trade-off between accelerating reaction kinetics and reducing process yield. Finding an optimal balance becomes crucial. Additionally, recycling of $ZnAc_2$, EG and GVL should be implemented to minimize the need for downstream purification and to reduce costs. Further, repolymerisation of the retrieved BHET product, which contains both monomers and dimers, into PET is necessary. This step will help evaluate whether additional purification steps to separate monomers and dimers are required.

Conflicts of interest

There are no conflicts to declare.

Acknowledgements

M. Schlüter thanks the German Federal Environmental Foundation (Deutsche Bundesstiftung Umwelt, DBU) for financial support.

References

1 S. A. Jabarin, Poly (ethylene terephthalate): Chemistry and preparation, *Polymeric Materials Encyclopedia*, 1996, vol. 4, pp. 6079–6085.
2 L. Bottenbruch, *Engineering Thermoplastics: Polycarbonates, Polycetals, Polyesters, Cellulose Esters*, Hanser Publisher, 1996.
3 E. M. Pearce and M. Lewin, *Handbook of fiber chemistry*, Marcel Dekker, 1998.
4 T. N. Tsironi, S. M. Chatzidakis and N. G. Stoforos, The future of polyethylene terephthalate bottles: Challenges and sustainability, *Packag. Technol. Sci.*, 2022, **35**, 317–325.
5 Statista Production of polyethylene terephthalate bottles worldwide from 2004 to 2021, 2021, https://www.statista.com/statistics/723191/production-of-polyethylene-terephthalate-bottles-worldwide/.
6 R. Becerril-Arreola and R. E. Bucklin, Beverage bottle capacity, packaging efficiency, and the potential for plastic waste reduction, *Sci. Rep.*, 2021, **11**, 3542.
7 S. H. Park and S. H. Kim, Poly (ethylene terephthalate) recycling for high value added textiles, *Fash. Text.*, 2014, **1**, 1.
8 A. M. Al-Sabagh, F. Z. Yehia, G. Eshaq, A. M. Rabie and A. E. ElMetwally, Greener routes for recycling of polyethylene terephthalate, *Egypt. J. Pet.*, 2016, **25**, 53–64.
9 E. Barnard, J. J. Rubio Arias and W. Thielemans, Chemolytic depolymerisation of PET: a review, *Green Chem.*, 2021, **23**, 3765–3789.
10 L. Rudolf, W. Gerhard and N. Clemens, Process for the recovery of dimethyl terephthalate from polyethylene terephthalate, utility patent, US3148208A, 1967.
11 M. N. Marathe, D. A. Dabholkar and M. K. Jain, Process for the recovery of dimethyl terephthalate from polyethylene terephthalate, *GB Pat.*, 2041916, 1980, vol. 2, p. 916.
12 R. E. Michel, Recovery of methyl esters of aromatic acids and glycols from thermoplastic polyester scrap using methanol vapor, *European Pat.*, 484963, 1992, vol. 484, p. 963.
13 C. Socrate and R. Vosa, Continuous process for the recovery of terephthalic acid from waste or used polyalkylene terephthalate polymers, *European Pat.*, 662466, 1995, vol. 662, p. 466.
14 J. Xin, Q. Zhang, J. Huang, R. Huang, Q. Z. Jaffery, D. Yan, Q. Zhou, J. Xu and X. Lu, Progress in the catalytic glycolysis of polyethylene terephthalate, *J. Environ. Manage.*, 2021, **296**, 113267.
15 G. P. Karayannidis, A. P. Chatziavgoustis and D. S. Achilias, Poly(ethylene terephthalate) recycling and recovery of pure terephthalic acid by alkaline hydrolysis, *Adv. Polym. Technol.*, 2002, **21**, 250–259.
16 A. Kumar and T. R. Rao, Kinetics of hydrolysis of polyethylene terephthalate pellets in nitric acid, *J. Appl. Polym. Sci.*, 2003, **87**, 1781–1783.
17 T. Yoshioka, T. Sato and A. Okuwaki, Hydrolysis of waste PET by sulfuric acid at 150°C for a chemical recycling, *J. Appl. Polym. Sci.*, 1994, **52**, 1353–1355.
18 T. Yoshioka, N. Okayama and A. Okuwaki, Kinetics of Hydrolysis of PET Powder in Nitric Acid by a Modified Shrinking-Core Model, *Ind. Eng. Chem. Res.*, 1998, **37**, 336–340.
19 T. Yoshioka, M. Ota and A. Okuwaki, Conversion of a Used Poly(ethylene terephthalate) Bottle into Oxalic Acid and Terephthalic Acid by Oxygen Oxidation in Alkaline Solutions at Elevated Temperatures, *Ind. Eng. Chem. Res.*, 2003, **42**, 675–679.
20 R. López-Fonseca, I. Duque-Ingunza, B. de Rivas, L. Flores-Giraldo and J. I. Gutiérrez-Ortiz, Kinetics of catalytic glycolysis of PET wastes with sodium carbonate, *Chem. Eng. J.*, 2011, **168**, 312–320.
21 R. López-Fonseca, I. Duque-Ingunza, B. de Rivas, S. Arnaiz and J. I. Gutiérrez-Ortiz, Chemical recycling of post-consumer PET wastes by glycolysis in the presence of metal salts, *Polym. Degrad. Stab.*, 2010, **95**, 1022–1028.
22 S. Baliga and W. T. Wong, Depolymerization of poly(ethylene terephthalate) recycled from post–consumer soft–drink bottles, *J. Polym. Sci., Part A: Polym. Chem.*, 1989, **27**, 2071–2082.
23 M. Ghaemy and K. Mossaddegh, Depolymerisation of poly(ethylene terephthalate) fibre wastes using ethylene glycol, *Polym. Degrad. Stab.*, 2005, **90**, 570–576.

24 M. E. Viana, A. Riul, G. M. Carvalho, A. F. Rubira and E. C. Muniz, Chemical recycling of PET by catalyzed glycolysis: Kinetics of the heterogeneous reaction, *Chem. Eng. J.*, 2011, **173**, 210–219.
25 J. R. Campanelli, M. R. Kamal and D. G. Cooper, Kinetics of glycolysis of poly(ethylene terephthalate) melts, *J. Appl. Polym. Sci.*, 1994, **54**, 1731–1740.
26 J.-W. Chen, L.-W. Chen and W.-H. Cheng, Kinetics of glycolysis of polyethylene terephthalate with zinc catalyst, *Polym. Int.*, 1999, **48**, 885–888.
27 B. Liu, X. Lu, Z. Ju, P. Sun, J. Xin, X. Yao, Q. Zhou and S. Zhang, Ultrafast Homogeneous Glycolysis of Waste Polyethylene Terephthalate via a Dissolution-Degradation Strategy, *Ind. Eng. Chem. Res.*, 2018, **57**, 16239–16245.
28 B. Liu, W. Fu, X. Lu, Q. Zhou and S. Zhang, Lewis Acid–Base Synergistic Catalysis for Polyethylene Terephthalate Degradation by 1,3-Dimethylurea/Zn(OAc) 2 Deep Eutectic Solvent, *ACS Sustainable Chem. Eng.*, 2019, **7**, 3292–3300.
29 N. H. Le, T. T. Ngoc Van, B. Shong and J. Cho, Low-Temperature Glycolysis of Polyethylene Terephthalate, *ACS Sustainable Chem. Eng.*, 2022, **10**, 17261–17273.
30 F. Kerkel, M. Markiewicz, S. Stolte, E. Müller and W. Kunz, The green platform molecule gamma-valerolactone – ecotoxicity, biodegradability, solvent properties, and potential applications, *Green Chem.*, 2021, **23**, 2962–2976.
31 S. Javed, J. Fisse and D. Vogt, Optimization and Kinetic Evaluation for Glycolytic Depolymerization of Post-Consumer PET Waste with Sodium Methoxide, *Polymer*, 2023, **15**, 687.
32 S. Javed, J. Fisse and D. Vogt, Kinetic Investigation for Chemical Depolymerization of Post-Consumer PET Waste Using Sodium Ethoxide, *Ind. Eng. Chem. Res.*, 2023, **62**, 4328–4336.
33 M. Schlüter, S. Bhutani, J. Bahr, K. Wohlgemuth and C. Held, Measurement and PCSAFT Modeling of the Solubility of the BHET Monomer, the BHET Dimer, and PET in Single Solvents, *J. Chem. Eng. Data*, 2024, **69**, 1326–1334.
34 S. Conroy and X. Zhang, Theoretical insights into chemical recycling of polyethylene terephthalate (PET), *Polym. Degrad. Stab.*, 2024, **223**, 110729.
35 M. Granatier, I. Schlapp-Hackl, H. Q. Lê, K. Nieminen, L. Pitkänen and H. Sixta, Stability of gamma-valerolactone under pulping conditions as a basis for process optimization and chemical recovery, *Cellulose*, 2021, **28**, 11567–11578.
36 W. Chen, Y. Yang, X. Lan, B. Zhang, X. Zhang and T. Mu, Biomass-derived γ-valerolactone: efficient dissolution and accelerated alkaline hydrolysis of polyethylene terephthalate, *Green Chem.*, 2021, **23**, 4065–4073.
37 M. Klinksiek, S. Baco, S. Leveneur, J. Legros and C. Held, Activity-Based Models to Predict Kinetics of Levulinic Acid Esterification, *ChemPhysChem*, 2023, **24**, e202200729.
38 A. M. Al-Sabagh, F. Z. Yehia, A. Eissa, M. E. Moustafa, G. Eshaq, A. M. Rabie and A. E. ElMetwally, Cu- and Zn-acetate-containing ionic liquids as catalysts for the glycolysis of poly(ethylene terephthalate), *Polym. Degrad. Stab.*, 2014, **110**, 364–377.
39 W. Chen, M. Li, X. Gu, L. Jin, W. Chen and S. Chen, Efficient glycolysis of recycling poly(ethylene terephthalate) via combination of organocatalyst and metal salt, *Polym. Degrad. Stab.*, 2022, **206**, 110168.